CHAPTER 6

Enhancer of zeste homolog-2 (EZH2) methyltransferase regulates transgelin/ smooth muscle-22 alpha expression in endothelial cells in response to interleukin-1 beta and transforming growth factor-beta 2

Monika Maleszewska, Rutger A.F. Gjaltema, Guido Krenning and Martin C. Harmsen

Department of Pathology and Medical Biology, University Medical Center Groningen, University of Groningen, The Netherlands

Cellular Signalling, 27, 1589–1596 (2015)

ABSTRACT

Smooth muscle-22α (SM22α), encoded by transgelin (*TAGLN*), is expressed in mesenchymal lineage cells, including myofibroblasts and smooth muscle cells. It is an F-actin binding protein that regulates the organization of actin cytoskeleton, cellular contractility and motility. SM22α is crucial for the maintenance of smooth muscle cell phenotype and its function. SM22α is also expressed in the processes of mesenchymal transition of epithelial (EMT) or endothelial cells (EndMT). The expression of *TAGLN*/SM22α is induced by transforming growth factor-β (TGFβ) signaling and enhanced by concomitant interleukin-1β (IL-1β) signaling. We investigated the epigenetic regulation of *TAGLN* expression by enhancer of zeste homolog-2 (EZH2), the methyltransferase of Polycomb, in the context of TGFβ2 and IL-1β signaling in endothelial cells. We demonstrate that the expression of EZH2 in endothelial cells was regulated by the inflammatory cytokine IL-1β. A decrease in both expression and activity of EZH2 led to an increase in *TAGLN* expression. Inhibition of EZH2 augmented TGFβ2-induced SM22α expression. The decrease of EZH2 levels in endothelial cells co-stimulated with IL-1β and TGFβ2 correlated with decreased H3K27me3 levels at the *TAGLN* proximal promoter. Moreover, the SM22α expression increased. Taken together, this suggests that EZH2 regulates the chromatin structure at the *TAGLN* promoter through tri-methylation of H3K27. EZH2 therefore acts as an epigenetic integrator of IL-1β and TGFβ2 signaling, providing an example of how cellular signaling can be resolved at the level of epigenetic regulation. Since IL-1β and TGFβ2 represent the pro-inflammatory and pro-fibrotic conditions during vascular fibroproliferative disease, we surmise that EZH2, as the molecule that integrates their signaling, could also be a promising target for development of future therapy.

INTRODUCTION

Smooth muscle-22α (SM22α2, transgelin), encoded by the gene *TAGLN*, is an evolutionarily conserved, F-actin binding protein, involved in the structural organization and stabilization of the actin cytoskeleton (1,2). The levels of SM22α determine cellularmotility (3) and contractility (4). SM22α/*TAGLN* is expressed in mesenchymal lineage cell types, such as fibroblasts or smooth muscle cells (SMC) (5). Its expression is altered upon differentiation processes (6,7), and it is induced by microenvironmental stimuli such as transforming growth factor-β (TGFβ) (8–10).

In particular, evidence shows that SM22α plays a crucial role in the maintenance of the SMC phenotype. Han *et al*. showed that depletion of SM22α results in a loss of SMC phenotype (1). Knock-out of SM22α in mice, although not lethal, results in decreased actin levels and reduced contractility of SMC (4). This knock-out also leads to an abnormal chondrogenic response of aortic SMC to injury and promotes vascular inflammation (11,12).

Given its necessity for the maintenance of the SMC phenotype, it is not surprising that SM22α is upregulated early in the course of the endothelial to mesenchymal transition (EndMT), a process inwhich endothelial cells differentiate into myofibroblast-like or SMC-like cells (8–10, 13–15). Postnatally, EndMT is a pathophysiological phenomenon that occurs in a pro-fibrotic environment (16–19). We previously investigated the influence of pro-fibrotic microenvironment on the progression of EndMT (10). Two major components of this environment are profibrotic factors from the TGFβ family and pro-inflammatory cytokines, such as interleukin-1β (IL-1β) (20,21). We demonstrated that IL-1β and TGFβ induce EndMT *in vitro* and that their signaling synergizes in the induction of expression of mesenchymal genes/proteins, an effect which was the most prominent in case of SM22α (10).

Polycomb is a family of chromatin modifying complexes, essential in the development and in adult life. Enhancer of zeste homolog-2 (EZH2) methyltransferase of the Polycomb repressive complex-2 (PRC2) is responsible for the deposition of the tri-methylation epigenetic mark on the lysine 27 of histone 3 (H3K27me3), which is associated with the maintenance of transcriptional repression (22,23). Polycomb function has been associated with inflammatory signaling. Tumor necrosis factor-α (TNFα) stimulation causes increased interaction between yin yang-1 (YY1) and PRC2 which, in satellite cells, enhances the formation of repressive chromatin on the developmentally important *Pax7* promoter (24). On the other hand, depletion of suppressor of zeste-12 homolog (SUZ12), another component of PRC2, enhances inflammatory response to IL-1β in epithelial cells [25).

The expression of SM22α was shown to be regulated at the epigenetic level by histone acetylation (26,27). We hypothesized that histone methylation by Polycomb family members epigenetically regulates SM22α expression in endothelial cells. EZH2 modulates endothelial gene expression and is important for endothelial function (28,29). As SM22α is synergistically induced by IL-1β and TGFβ2 in endothelial cells, we investigated the influence of IL-1β and TGFβ2 on the expression of EZH2 and the downstream role of EZH2 and H3K27me3 inmediating the effects of IL-1β and TGFβ2 and in the regulation of *TAGLN*/SM22α expression in endothelial cells.

MATERIALS AND METHODS

Cell culture
Human Umbilical Vein Endothelial Cells (HUVEC, Lonza) were used between passages 5 and 8. Cells were cultured in gelatin-coated dishes in endothelial cell medium (ECM) prepared as described before (10), but with 5.5 mM glucose and 10% heat-inactivated fetal calf serum (FCS; Lonza) for regular culture, and 5% heat-inactivated FCS in all experiments involving stimulations. IL-1β and TGFβ2 (Peprotech, #200-01B and #100-35B, respectively) were used at concentration of 10 ng/ml each. The specific EZH2 inhibitor GSK126 (30) (Cellagen Technology, C4126-2s) was dissolved in DMSO and used at 1 μM final concentration. Equal volume of DMSO was used in control medium. All stimulations were performed for 4 days, and media were refreshed daily.

Lentiviral transduction
Human Embryonic Kidney (HEK) cells were cultured in 10% FCS DMEM (Lonza), 2 mM L-glutamine (Lonza), 1% penicillin/streptomycin (Gibco). HEK were transfected with following plasmids: pLKO.1-shEZH2 or pLKO.1-SCR, pCMVΔR8.91 (gag-pol 2nd generation packaging plasmid) and pVSV-G (envelope plasmid) using Endofectin™-Lenti (Gene Copoeia, EFL-1001-01). A day after transfection, virus collection was commenced in 10% FCS ECM medium. Supernatants were collected 2 times at 24 h intervals, filtered through 0.45 μm filters and applied to 30% confluent HUVEC cultures. Every first transduction was performed with addition of polybrene at concentration of 4 μg/ml. Cells were allowed to proliferate for another 3 days before they were selected in 10% FCS ECM with 2 μg/ml of puromycin (Invitrogen). Surviving cells were allowed to proliferate for another 24 h and were used for downstream analyses at day 7 from the first transduction.

Real-time PCR
Cells were lysed either with TriZOL (Invitrogen) or RNA-Bee (TELTEST, Inc.) reagents. RNA was isolated in accordance to standard procedures. Briefly, chloroform was added and samples were shaken and incubated on ice for 10 min, then centrifuged. The aqueous phase was collected and RNA was precipitated with 2-propanol, washed 2 times with ice-cold 75% ethanol, dried and suspended in RNAse-free water. Concentrations were determined by spectrophotometry (NanoDrop, ThermoScientific). cDNA synthesis was performed using RevertAid™ First Strand cDNA Synthesis Kit (ThermoScientific). 10 ng of cDNA, calculated based on the RNA input, was used per a single Real-time PCR reaction (20 ng per reaction in the IL1B PCR). Real-time PCR was performed using SYBR-Green chemistry (BioRad or Roche) with the ViiA7 Real Time PCR system (Applied Biosystems), and data were analyzed using ViiA7 software (Applied Biosystems). Downstream analysis was performed in Excel. Geometrical mean of *ACTB* and *GAPDH* Ct values, or only *GAPDH* Ct values (consistent within an experiment) were used for normalization (ΔCt). Fold change over control samples was calculated using ΔΔCt method. The following primers were used (5' to 3'): *ACTA2* Forward: CTGTTCCAGCCAATCCTTCAT, Reverse: TCATGATGCTGTTGTAGGTGGT; *ACTB* Forward: CCAACCGCGAGAAGATGA, Reverse: CCAGAGGCGTACAGGGATAG; *CNN1*

Forward: CCAACCATACACAGGTGCAG, Reverse: TCACCTTGTTTCCTTTCGTCTT; *EZH2* Forward: GCGAAGGATACAGCCTGTGCACA, Reverse: AATCCAAGTCACTGGTCACCGAAC; *FN1* Forward: TCAACTCACAGCTTCTCCAA, Reverse: TTGATCCCAAACCAAATCTT; *IL1B* Forward: AAGCTGGAATTTGAGTCTGC, Reverse: ACACAAATTGCATGGTGAAG; *GAPDH* Forward: AGCCACATCGCTCAGACAC, Reverse: GCCCAATACGACCAAATCC; *TAGLN* Forward: CTGAGGAC TATGGGGTCATC, Reverse: TAGTGCCCATCATTCTTGGT.

Western blotting

Cells were lysed with RIPA buffer (ThermoScientific) supplemented with proteinase inhibitor cocktail and phosphatase inhibitor cocktails-2 and -3 (all from Sigma Aldrich) and stored at−80 °C. Prior to Western blotting, lysates were thawed, sonicated and centrifuged. Protein concentration in the supernatants was measured using Bio-Rad DC™ protein concentration assay (Bio-Rad). Samples were loaded onto 10% polyacrylamide gels and electrophoresis was performed. Transfer was performed onto nitrocellulose membranes at 100 V. Membranes were blocked with Odyssey Blocking Buffer (Li-COR Biosciences) diluted 1:1 with Tris-buffered saline (TBS) for 1 h at room temperature (RT), then incubatedwith primary antibodies dissolved in Odyssey Blocking Buffer diluted 1:1 with TBS at 4 °C overnight, at a rocking platform. Next day the membranes were washed 3 times with TBS 0.1% Tween-20 and incubatedwith secondary antibodies in Odyssey Blocking Buffer diluted 1:1with TBS 1 h at RT, mixing. Then theywerewashed 3 timeswith TBS 0.1% Tween and 3 times with TBS, and scanned using the Odyssey scanner (Li-COR Biosciences). Digital images of the membranes were converted into grayscale images using the Odyssey software (Li-COR Biosciences). These images were used in the densitometry analysis with TotalLab 120 software (Nonlinear Dynamics). The following antibodies were used: EZH2 (1:1000, Cell Signaling, 5246), GAPDH (1:1000, Abcam, ab9485 or ab9484), phospho-SMAD2 (1:500, Cell Signaling, 3108), SM22α (1:1000, Abcam, ab14106), antirabbit IgG IRDye-680LT (1:10 000, Li-COR Biosciences, 926-68021), anti-mouse IgG IRDye-800CW (1:10 000, Li-COR Biosciences, 926- 32210).

Chromatin immunoprecipitation

HUVEC treated with IL-1β, TGFβ2, or IL-1β and TGFβ2 (or control) were washed with PBS, harvested with trypsine (MP Biomedicals, LLC), counted and fixed with 1% formaldehyde. The fixing solution was neutralized with glycine solution (125 mM), cells were washed three times with PBS and cell pellets were stored at −80 °C. Prior to ChIP, cell pellets were thawed and lysed on ice for 20 min with SDS lysis buffer (1% SDS, 50 mM Tris–HCl pH 8.0, 10 mM EDTA) supplemented with proteinase inhibitor cocktail and PMSF (Sigma Aldrich). The chromatin was fragmented by sonication with a Bioruptor® device (Diagenode) and cleared by centrifugation at 13000 RPM for 10 min at 4 °C. The chromatin was diluted tenfold with RIPA buffer (0.1% SDS, 0.1% Na-deoxycholate, 1% Triton-X100, 1 mM EDTA, 10 mM Tris–HCl pH 7.5, 140 mM NaCl, 0.5 mM EGTA) supplemented with proteinase inhibitor cocktail and PMSF. Then, 40 µl Dynabeads® Protein-A (Life Technologies) were coated with 5 µg antibodies against H3K27me3 (Millipore, 07-449) or normal rIgG (Abcam, ab46540) as a control, and incubated overnight at 4 °C with diluted chromatin of 0.8×10^6 cells. The following day,

the beads were washed three times with ice cold PBS and the remaining complexes were eluted with a solution of 100 mM NaHCO3 and 1% SDS. After reversing the crosslinks in the elutes with NaCl at 62 °C and treating with RNAse (Roche) and Proteinase K (Roche), the DNA fragments were purified by using a QIAquick PCR purification kit (Qiagen) and quantified by Real-time PCR with SYBR Green (Roche) and primers that amplify regions in the proximal promoters. Data is represented as fold enrichment over control rIgG values. The following primers were used (5' to 3'): *IL1B* Forward: GGACATCAACTGCACAACGA, Reverse: ATGGAAGGGCAAGGAGTAGC; *TAGLN* Forward: TCTCCAAAGCATGCAGAGAA, Reverse: GACTCCACACAGGCTCCATA.

Immunofluorescence
Cells were cultured in 24-well plates. After 4 days of stimulation, cells were washed with PBS and fixed in 2% paraformaldehyde in PBS for 30 min at RT. Cells were washed with PBS, permeabilized with 1% Triton-X100 in PBS for 10 min at RT, washed with PBS and blocked with 10% donkey serum in PBS for 30 min at RT. Subsequently, cells were incubated with primary antibodies diluted in 10% donkey serum in PBS overnight at 4 °C, rocking. Controls were incubated with 10% donkey serum in PBS. Subsequently, cells were washed 3 times in PBS 0.05% Tween-20, 1 time in PBS and then incubated with secondary antibodies in 10% donkey serum in PBS with DAPI (1:5000), for 1 h at RT, rocking. Cells were then washed with PBS 0.05% Tween, and in PBS. Wells were filled with 0.5 ml of PBS and plates were scanned with TissueFAXS microscope (TissueGnostics). Images were further analyzed with TissueQuest 4.0.1.0127 software (TissueGnostics). DAPI nuclear staining was used to identify cells. For better visualization the brightness of the images included in the figures was enhanced in a linearmanner and to the same extend in each image (Adobe Photoshop CS6). The following antibodies were used: SM22α (1:500, Abcam, ab14106), anti-rabbit IgG AlexaFluor-555 (1:500, Life Technologies, A31572).

ELISA
Three hours prior to sampling, medium of HUVEC was refreshed. Collected culture supernatants were filtered (0.2 µm), aliquotted and stored at −80 °C. The concentration of secreted IL-1β was determined using the human IL-1 beta DuoSet ELISA kit (R&D Systems, Oxon, UK) according to the manufacturer's protocol. Concentrations of two-fold serially diluted samples were determined by comparison to the IL-1β concentration standard curve, fit using a four parameter logistic (4-PL) curve-fit. The cells were lysed and total DNA was measured with CyQuant kit (Invitrogen). Total amount of IL-1β per well was calculated based on themeasured IL-1β concentrations, andwas normalized to the amount of DNA in a well, to normalize for differences in cell numbers.

Statistical analysis
Downstream calculations were performed using Excel, statistical analysis and plotting were executed in GraphPad Prism 4 or 5 (GraphPad Software, La Jolla, CA). Graphs present mean values with standard error of the mean of at least 3 independent experiments. *t*-test or 1-way ANOVA with Tukey post-hoc comparisons between all pairs of means were performed where appropriate. Probability values lower than 0.05

were considered to indicate significant difference between means.

RESULTS

IL-1β suppresses expression of EZH2 in endothelial cells

Previously, we demonstrated that co-stimulation of endothelial cells with IL-1β and TGFβ2 leads to a synergistical induction of gene expression of *TAGLN* within day 5 of stimulation. Here, we confirmed that a similar synergistical upregulation of SM22α occurred at day 4 of stimulation (Fig. 1a). We evaluated the expression of *EZH2* at the same time point. Stimulation with IL-1β, or with IL-1β and TGFβ2 together, decreased the gene expression of *EZH2* to a similar level (Fig. 1b), however TGFβ2 alone did not affect *EZH2* expression, which shows that the change in gene expression of *EZH2* depended solely on IL-1β signaling. The protein expression of EZH2 also decreased under IL-1β treatment, but not under TGFβ2 treatment (Fig. 2a and b).

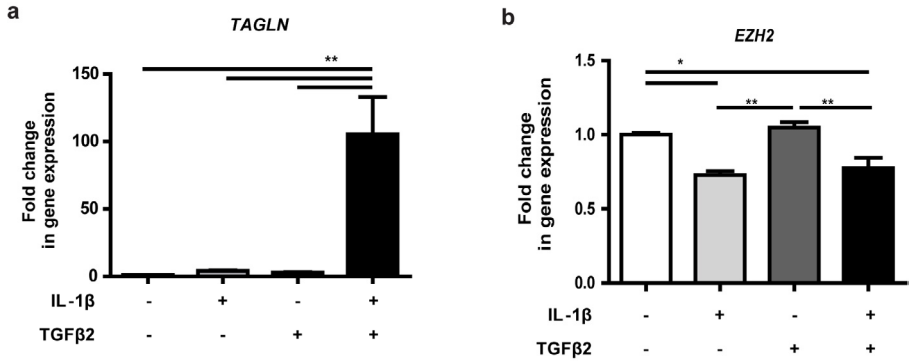

Figure 1. Regulation of the expression of *TAGLN* and *EZH2* by IL-1β and TGFβ2.
Cells were treated daily with 10 ng/ml of IL-1β, TGFβ2 or both. a: Fold change in gene expression of *TAGLN*. b: Fold change in gene expression of *EZH2*. *p<0.05, **p<0.01, ***p<0.001.

Treatment of HUVEC with IL-1β upregulated *IL1B* gene and protein expression (Fig. 3a and c). As IL1B is a putative EZH2-regulated gene (28), we speculated that IL-1β and EZH2 would form a regulatory feedback loop in endothelial cells. The decrease of EZH2 in IL-1β-stimulated HUVEC could lead to decrease of H3K27me3 at *IL1B* promoter and hence to an increase in IL1B/IL-1β expression. However, the inhibition of EZH2 activity with GSK126 increased IL1B expression to a lower extend than IL-1β-stimulation (Fig. 3b). Furthermore, despite a significant increase in *IL1B* gene expression, the protein levels of IL-1β only tended to increase upon inhibition of EZH2 (Fig. 3d). Finally, IL-1β, TGFβ2, or the combination, did not affect the abundance of H3K27me3 at the IL1B promoter
(Fig. 3e). Altogether, this suggests that EZH2 activity does not directly regulate the activity of the IL1B promoter in response to IL-1β and/or TGFβ2.

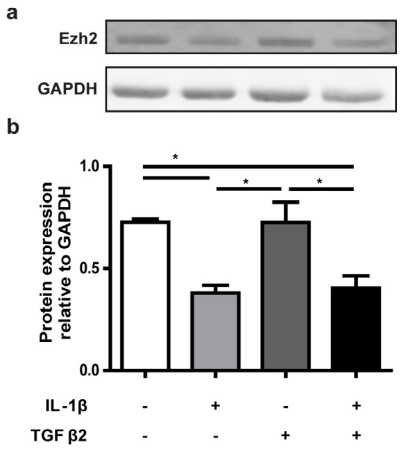

Figure 2. Regulation of the expression of EZH2 protein by IL-1β and TGFβ2.
Cells were treated daily with 10 ng/ml of IL-1β, TGFβ2 or both. a: Representative Western blotting images showing the expression of EZH2, GAPDH serves as loading control. b: Fold change in protein expression of EZH2. *p<0.05.

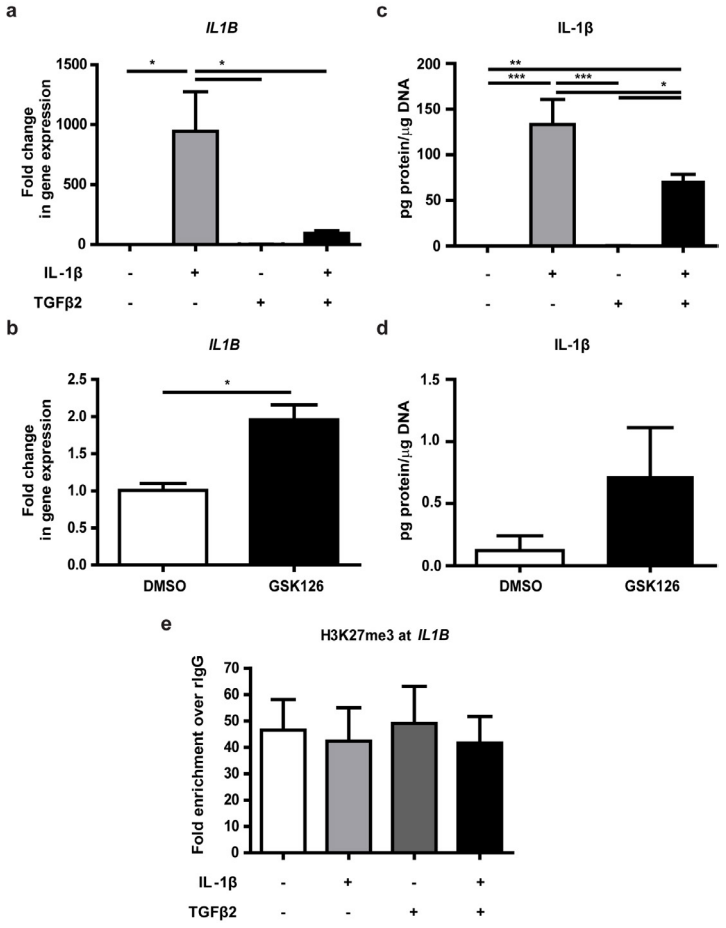

Figure 3. IL-1β positive feedback regulation does not require EZH2.
HUVEC were stimulated daily for 4 days with 10ng/ml IL-1β, 10ng/ml TGFβ2, or both, or with the GSK126 EZH2 inhibitor. a and b: Fold change in *IL1B* expression. c and d: IL-1β protein levels determined by ELISA. e: H3K27me3 abundance levels at the proximal promoter of *IL1B*, presented as fold enrichment over respective rabbit IgG control pull downs. *p<0.05.

EZH2 regulates SM22α expression in endothelial cells

Next, we evaluated the putative contribution of EZH2 to the regulation of *TAGLN*/SM22α expression. Both inhibition of EZH2 activity with GSK126 and knock-down of EZH2with shRNA increased the expression of *TAGLN* in HUVEC (Fig. 4a and b). We also observed upregulation of other mesenchymal genes *ACTA2*, *CNN1* and *FN1* upon inhibition of EZH2 activity (Suppl. Fig. 1). However, shRNA-mediated EZH2-depleted cells had an increased expression of *ACTA2*, but the expression of *CNN1* and *FN1* was not increased (Suppl. Fig. 2). Protein expression analysis of EZH2-depleted HUVEC confirmed the knock-down of *EZH2* and the increase of SM22α expression (Fig. 4c, d and e).

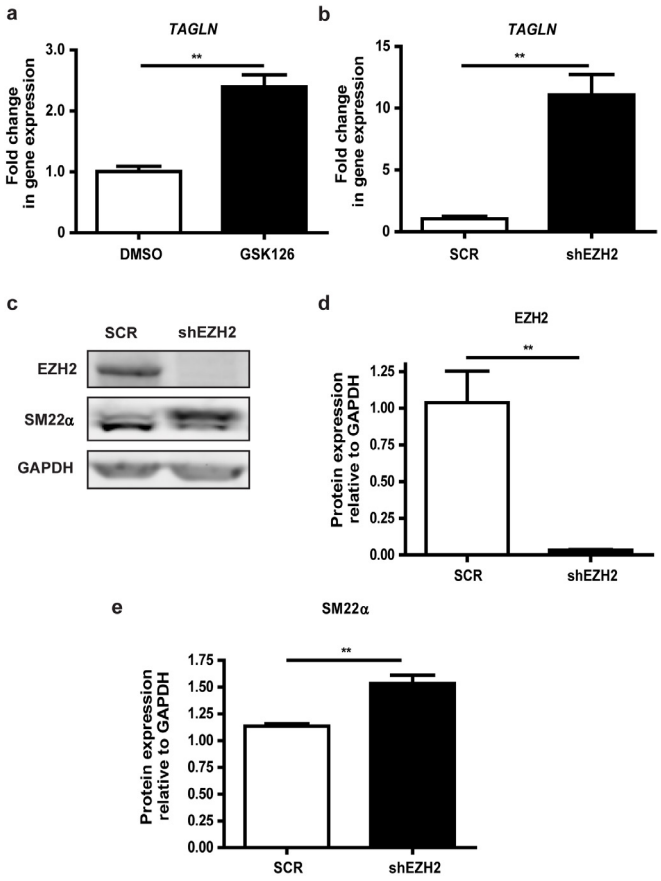

Figure 4. EZH2 regulates the expression of TAGLN/SM22α.

a: Cells were treated with 1μM EZH2 inhibitor GSK126 daily for 4 days. Fold change in gene expression is depicted. b through c: Cells were depleted of EZH2 by means of lentiviral overexpression of shRNA. b: Fold change in gene expression of TAGLN. c: Representative Western blotting images showing the expression of EZH2 and SM22α protein, GAPDH serves as loading control. d and e: Densitometry results of the Western blotting data showing the protein expression of EZH2 and SM22α, normalized to GAPDH levels. **p<0.01.

Inhibition of EZH2 activity potentiates TGFβ2-induced expression of SM22α

TGFβ signaling induces SM22α expression in fibrotic tissue and during the process of EndMT. We assessed if the inhibition of EZH2 enhanced the increase of SM22α expression induced by TGFβ2. Separate treatment with the EZH2 inhibitor GSK126 or with TGFβ2 both tended to increase SM22α expression. The combination of both GSK126 and TGFβ2 additively increased the expression of SM22α (Fig. 5a and b). Treatment with GSK126 and TGFβ2 together also increased the phosphorylation levels of mothers against decapentaplegic homolog-2 (SMAD2) (Suppl. Fig. 3). Immunofluorescent staining confirmed the induction of SM22α expression by the co-treatment with GSK126 and TGFβ2 (Fig. 5c and d).

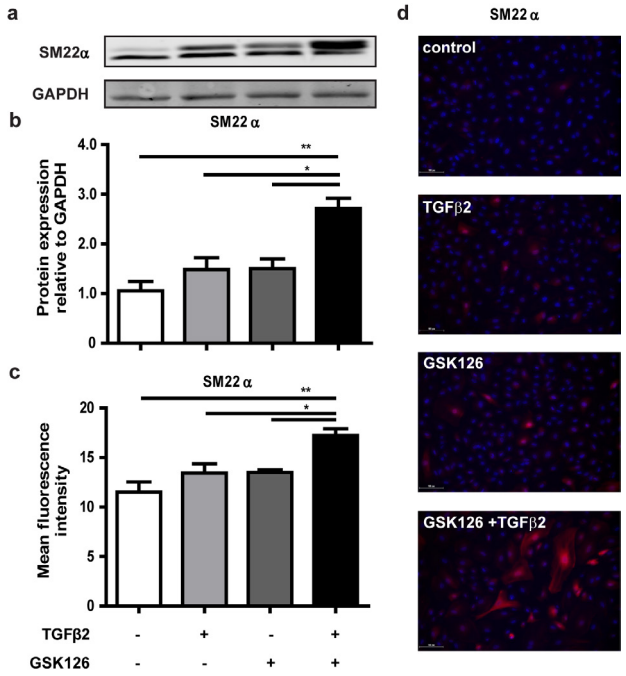

Figure 5. Inhibition of EZH2 activity enhances the TGFβ2-induced expression of SM22α.
HUVEC were treated with the EZH2 inhibitor GSK126 (1μM), or 10ng/ml TGFβ2, or combination of both, daily for 4 days. a: Representative Western blotting results of SM22α expression; GAPDH served as loading control. b: Expression of SM22α derived through densitometry of Western blotting data, normalized to the GAPDH loading control. c: Expression of SM22α based on the measurement of mean fluorescence intensity (MFI) of SM22α staining. d: Representative images of SM22α staining (red), 20x magnification, bars indicate 100μm. Blue – DAPI. *p<0.05, **p<0.01.

The IL-1β and TGFβ2-co-induced SM22α expression is associated with decreased H3K27me3 levels at the *TAGLN*/SM22α promoter

We next checked if the decrease in *EZH2* expression upon IL-1β (and concomitant TGFβ2) treatment would result in changes in H3K27me3 levels at *TAGLN* promoter and

coincide with the change in *TAGLN*/SM22α expression. Co-treatment with IL-1β and TGFβ2 decreased H3K27me3 levels at the *TAGLN* promoter (Fig. 6a). The lowest levels of H3K27me3 at the *TAGLN* promoter corresponded with the highest level of SM22α expression under co-treatment conditions (Fig. 6b and c).

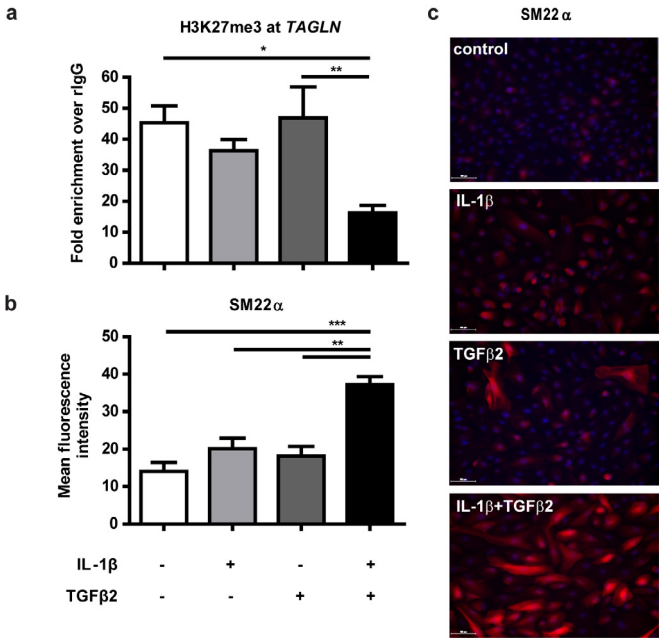

Figure 6. The IL-1β and TGFβ2 decrease H3K27me3 levels at the *TAGLN*/SM22α promoter.
HUVEC were stimulated daily for 4 days with 10ng/ml IL-1β, 10ng/ml TGFβ2, or both. a: H3K27me3 abundance levels at the proximal promoter of *TAGLN*, presented as fold enrichment over respective rabbit IgG control pull downs. b: Representative images of SM22α staining (red), 20x magnification, bars indicate 100μm. Blue – DAPI. c: Levels of SM22α expression, derived from mean fluorescence intensity of its staining. *p<0.05, **p<0.01, ***p<0.001.

DISCUSSION

We demonstrated that, in endothelial cells, the expression of *TAGLN*/SM22α is regulated at the epigenetic level by the Polycomb methyltransferase EZH2. Both expression and activity of EZH2 co-determine the expression levels of *TAGLN*/SM22α in endothelial cells. Our *in vitro* investigation suggests that *in vivo* EZH2 might partake in the regulation of *TAGLN* in response to its physiological pro-fibrotic and proinflammatory inducers such as TGFβ and IL-1β. The decrease in EZH2 levels upon IL-1β and TGFβ2 stimulation, and the resulting decrease of repressive modification H3K27me3 at the *TAGLN* promoter, could be the mechanism for activation of *TAGLN* promoter leading to the enhanced expression of *TAGLN*/SM22α.

EZH2 can therefore be a downstream effector that integrates the signaling pathways of IL-1β and TGFβ2. This mechanism could be crucial in the regulation of the SM22α expression in a pro-fibrotic inflammatory microenvironment and during the process of EndMT.

Several epigenetic mechanisms involving Polycomb play a role in mediating the transcriptional effects of pro-inflammatory signaling. Hahn *et al*. reported changes in DNA methylation of Polycomb target genes in epithelial cells in an inflammatory bowel disease model (31). De Santa *et al*. linked inflammation to the function of an H3K27me3 demethylase Jmjd3 (32), which could be a complementary mechanism (to EZH2-mediated H3K27me3 deposition) for modulation of H3K27me3 levels. Palacios and co-workers have shown that TNFα changes the activity of EZH2, but not *EZH2* expression itself (24). Therefore, to the best of our knowledge, the repressive effect of IL-1β on *EZH2* expression, which we observed, has not been reported before.

We showed previously that the synergistic increase in *TAGLN*/SM22α expression upon IL-1β and TGFβ2 co-stimulation depends on NFκB activation (10). However, we did not observe a rescue of the *EZH2* expression upon inhibition of the canonical NFκB pathway in our initial experiments (data not shown), therefore the effects of IL-1β and TGFβ2 on EZH2 activity did not seem to depend on NFκB signaling.

TGFβ2 signaling could also contribute to the regulation of EZH2 activity, as the H3K27me3 levels at the *TAGLN* promoter decreased the most upon IL-1β and TGFβ2 co-stimulation. Wang *et al*. proposed that TGFβ-activated SMAD2 and SMAD4 displace EZH2 from Il9 locus in Th9 T-cells (33). This seems to corroborate our results, as the TGFβ2- activated SMAD2 (pSMAD2) could possibly facilitate the removal of EZH2 from different nuclear loci, including the promoter region of *TAGLN* (which is a TGFβ/SMAD2-inductive gene). Therefore, the TGFβ2-signaling, in particular through SMAD2 activation, could add to the IL-1β-mediated decrease of EZH2 expression and thereby explain the lowest levels of the H3K27me3 histone mark and the highest expression levels of SM22α under IL-1β and TGFβ2 co-stimulation conditions.

Moreover, by inhibiting EZH2 activity we were able to enhance the TGFβ2-induced expression of SM22α. Interestingly, EZH2 inhibition had similar effect on activation of SMAD2. Vella *et al.* observed increased expression of TGFβ in tissue with decreased EZH2 levels and in cells upon inhibition of EZH2 (34). Such autocrine production of TGFβ could explain our observation of increased SMAD2 activation by TGFβ2 upon inhibition of EZH2 in HUVEC.

Our study therefore describes a new level of integration of IL-1β and TGFβ2 signaling, which occurs at the level of EZH2. Even if the mechanisms of IL-1β- and of TGFβ2-exerted regulation of *EZH2* are distinct (decrease in expression versus displacement), eventually they could act cooperatively, as illustrated by the decreasing levels of H3K27me3 at *TAGLN* promoter. This interaction in a pro-fibrotic milieu might be required to efficiently alter histone methylation, and to thereby change the promoter activity of fibrosis-related genes, such as *TAGLN*.

Moreover, this regulation mechanism of *TAGLN* promoter by EZH2 under influence of IL-1β and TGFβ2 further shows that not only global, but also local activity of EZH2 at promoters of specific genes can be guided by signaling pathways.

Decreased EZH2 expression has been observed before in the course

of differentiation of adult stem/progenitor cells and correlated with changes in expression of EZH2-regulated genes (35,36). On the other hand, increased expression of EZH2 is often seen in highly proliferating cells (37). EZH2 expression levels also influence the differentiation decisions in human bone marrow-derived mesenchymal stem cells (38). In differentiating murine embryonic stem cells (mESCs) the expression of developmental genes is regulated by PRC2 activity and its localization to specific loci through interaction with JARID2 (39). Recent report showed that in mESCs PRC2 binds the nucleosome-free CpG islands in proximity of transcriptionally inactive genes, to maintain their repression (23). These reports show that EZH2 and Polycomb function can be regulated by changes in their abundance and activity, to help to guide the differentiation processes of the cells. This suggests that the decrease in EZH2 expression upon IL-1β could have similar functionsin EndMT.

The expression of SM22α/*TAGLN* is regulated at the epigenetic level through histone acetylation (26,27). Here we show that EZH2-mediated histone methylation (H3K27me3) is involved in the regulation of TAGLN promoter and *TAGLN* expression. *TAGLN* has been used by others as a model gene to study the regulation of smooth-muscle cell (SMC)-specific genes (26,27). SM22α/TAGLN is also necessary for themaintenance of the phenotype and for proper function of SMC (1,11). In our previous work, increased expression of SM22α/*TAGLN* was an early-induced indicator of EndMT (10). Our results therefore suggest that EZH2, by integrating the IL-1β and TGFβ2 signaling at the level of *TAGLN* regulation, could contribute to the progression of transdifferentiation process of EndMT.

Our results suggest that SM22α/*TAGLN* expression in response to IL-1β and TGFβ2 in endothelial cells is co-regulated at the chromatin level through histone methylation (H3K27me3), most likely through regulation of the abundance of the Polycomb methyltrasferase EZH2. EZH2 appears to integrate and mediate the IL-1β and TGFβ signaling at the epigenetic level. This further suggests a role for EZH2 in the responses of endothelial cells to the microenvironment, in particular to the pro-fibrotic and pro-inflammatory cues driving the process of EndMT.

ACKNOWLEDGEMENTS

We would like to thank Dr. V. van den Boom and Prof. Dr. J.J. Schuringa (Dept. Experimental Hematology, University Medical Center Groningen) for the shEZH2 and scrambled control plasmids used in this study. Imaging was performed at the UMCG Imaging Center (UMIC), supported by theNetherlands Organization forHealth Research and Development (ZonMW, #40-00506-98-9021). The authors thankfully acknowledge the financial support of the Netherlands Institute for Regenerative Medicine (NIRM, #FES0908; M.C.H.). This work was additionally supported by the Groningen University Institute for Drug Exploration (GUIDE; G.K. andM.C.H.), the ZonMW/Netherlands Organization for Scientific Research (NWO) Innovational Research Incentive (#916.11.022; G.K.) and the Jan-Kornelis de Cock foundation (M.M.). Funding bodies had no role in study design, data collection or analysis, decision to publish, or preparation of the manuscript. The authors declare no conflicts of interests.

REFERENCES

1. Han, M., Dong, L.H., Zheng, B., Shi, J.H., Wen, J.K. and Cheng, Y. (2009) Smooth muscle 22 alpha maintains the differentiated phenotype of vascular smooth muscle cells by inducing filamentous actin bundling. Life sciences, 84, 394-401.
2. Fu, Y., Liu, H.W., Forsythe, S.M., Kogut, P., McConville, J.F., Halayko, A.J., Camoretti-Mercado, B. and Solway, J. (2000) Mutagenesis analysis of human SM22: characterization of actin binding. Journal of applied physiology, 89, 1985-1990.
3. Thompson, O., Moghraby, J.S., Ayscough, K.R. and Winder, S.J. (2012) Depletion of the actin bundling protein SM22/transgelin increases actin dynamics and enhances the tumourigenic phenotypes of cells. BMC Cell Biol, 13, 1.
4. Zeidan, A., Sward, K., Nordstrom, I., Ekblad, E., Zhang, J.C., Parmacek, M.S. and Hellstrand, P. (2004) Ablation of SM22alpha decreases contractility and actin contents of mouse vascular smooth muscle. FEBS Lett, 562, 141-146.
5. Lawson, D., Harrison, M. and Shapland, C. (1997) Fibroblast transgelin and smooth muscle SM22alpha are the same protein, the expression of which is down-regulated in many cell lines. Cell motility and the cytoskeleton, 38, 250-257.
6. Li, L., Miano, J.M., Cserjesi, P. and Olson, E.N. (1996) SM22 alpha, a marker of adult smooth muscle, is expressed in multiple myogenic lineages during embryogenesis. Circulation research, 78, 188-195.
7. Duband, J.L., Gimona, M., Scatena, M., Sartore, S. and Small, J.V. (1993) Calponin and SM 22 as differentiation markers of smooth muscle: spatiotemporal distribution during avian embryonic development. Differentiation; research in biological diversity, 55, 1-11.
8. Krenning, G., Moonen, J.R., van Luyn, M.J. and Harmsen, M.C. (2008) Vascular smooth muscle cells for use in vascular tissue engineering obtained by endothelial-to-mesenchymal transdifferentiation (EnMT) on collagen matrices. Biomaterials, 29, 3703-3711.
9. Moonen, J.R., Krenning, G., Brinker, M.G., Koerts, J.A., van Luyn, M.J. and Harmsen, M.C. (2010) Endothelial progenitor cells give rise to pro-angiogenic smooth muscle-like progeny. Cardiovascular research, 86, 506-515.
10. Maleszewska, M., Moonen, J.R., Huijkman, N., van de Sluis, B., Krenning, G. and Harmsen, M.C. (2013) IL-1beta and TGFbeta2 synergistically induce endothelial to mesenchymal transition in an NFkappaB-dependent manner. Immunobiology, 218, 443-454.
11. Shen, J., Yang, M., Jiang, H., Ju, D., Zheng, J.P., Xu, Z., Liao, T.D. and Li, L. (2011) Arterial injury promotes medial chondrogenesis in Sm22 knockout mice. Cardiovascular research, 90, 28-37.
12. Shen, J., Yang, M., Ju, D., Jiang, H., Zheng, J.P., Xu, Z. and Li, L. (2010) Disruption of SM22 promotes inflammation after artery injury via nuclear factor kappaB activation. Circulation research, 106, 1351-1362.
13. Arciniegas, E., Sutton, A.B., Allen, T.D. and Schor, A.M. (1992) Transforming growth factor beta 1 promotes the differentiation of endothelial cells into smooth muscle-like cells in vitro. J Cell Sci, 103 (Pt 2), 521-529.
14. Frid, M.G., Kale, V.A. and Stenmark, K.R. (2002) Mature vascular endothelium can give rise to smooth muscle cells via endothelial-mesenchymal transdifferentiation: in vitro analysis. Circulation research, 90, 1189-1196.
15. Ishisaki, A., Hayashi, H., Li, A.J. and Imamura, T. (2003) Human umbilical vein endothelium-derived cells retain potential to differentiate into smooth muscle-like cells. J Biol Chem, 278, 1303-1309.
16. Zeisberg, E.M., Tarnavski, O., Zeisberg, M., Dorfman, A.L., McMullen, J.R., Gustafsson, E., Chandraker, A., Yuan, X., Pu, W.T., Roberts, A.B. et al. (2007) Endothelial-to-mesenchymal transition contributes to cardiac fibrosis. Nat Med, 13, 952-961.
17. Zeisberg, E.M., Potenta, S.E., Sugimoto, H., Zeisberg, M. and Kalluri, R. (2008) Fibroblasts in kidney fibrosis emerge via endothelial-to-mesenchymal transition. Journal of the American Society of Nephrology : JASN, 19, 2282-2287.

18. Hashimoto, N., Phan, S.H., Imaizumi, K., Matsuo, M., Nakashima, H., Kawabe, T., Shimokata, K. and Hasegawa, Y. (2010) Endothelial-mesenchymal transition in bleomycin-induced pulmonary fibrosis. American journal of respiratory cell and molecular biology, 43, 161-172.

19. Krenning, G., Zeisberg, E.M. and Kalluri, R. (2010) The origin of fibroblasts and mechanism of cardiac fibrosis. J Cell Physiol, 225, 631-637.

20. Bujak, M., Dobaczewski, M., Chatila, K., Mendoza, L.H., Li, N., Reddy, A. and Frangogiannis, N.G. (2008) Interleukin-1 receptor type I signaling critically regulates infarct healing and cardiac remodeling. Am J Pathol, 173, 57-67.

21. Bujak, M. and Frangogiannis, N.G. (2009) The role of IL-1 in the pathogenesis of heart disease. Archivum immunologiae et therapiae experimentalis, 57, 165-176.

22. Bracken, A.P. and Helin, K. (2009) Polycomb group proteins: navigators of lineage pathways led astray in cancer. Nature reviews. Cancer, 9, 773-784.

23. Riising, E.M., Comet, I., Leblanc, B., Wu, X., Johansen, J.V. and Helin, K. (2014) Gene silencing triggers polycomb repressive complex 2 recruitment to CpG islands genome wide. Mol Cell, 55, 347-360.

24. Palacios, D., Mozzetta, C., Consalvi, S., Caretti, G., Saccone, V., Proserpio, V., Marquez, V.E., Valente, S., Mai, A., Forcales, S.V. et al. (2010) TNF/p38alpha/polycomb signaling to Pax7 locus in satellite cells links inflammation to the epigenetic control of muscle regeneration. Cell stem cell, 7, 455-469.

25. Turgeon, N., Blais, M., Delabre, J.F. and Asselin, C. (2013) The histone H3K27 methylation mark regulates intestinal epithelial cell density-dependent proliferation and the inflammatory response. J Cell Biochem, 114, 1203-1215.

26. Qiu, P. and Li, L. (2002) Histone acetylation and recruitment of serum responsive factor and CREB-binding protein onto SM22 promoter during SM22 gene expression. Circulation research, 90, 858-865.

27. Qiu, P., Ritchie, R.P., Gong, X.Q., Hamamori, Y. and Li, L. (2006) Dynamic changes in chromatin acetylation and the expression of histone acetyltransferases and histone deacetylases regulate the SM22alpha transcription in response to Smad3-mediated TGFbeta1 signaling. Biochem Biophys Res Commun, 348, 351-358.

28. Dreger, H., Ludwig, A., Weller, A., Stangl, V., Baumann, G., Meiners, S. and Stangl, K. (2012) Epigenetic regulation of cell adhesion and communication by enhancer of zeste homolog 2 in human endothelial cells. Hypertension, 60, 1176-1183.

29. Lu, C., Han, H.D., Mangala, L.S., Ali-Fehmi, R., Newton, C.S., Ozbun, L., Armaiz-Pena, G.N., Hu, W., Stone, R.L., Munkarah, A. et al. (2010) Regulation of tumor angiogenesis by EZH2. Cancer cell, 18, 185-197.

30. McCabe, M.T., Ott, H.M., Ganji, G., Korenchuk, S., Thompson, C., Van Aller, G.S., Liu, Y., Graves, A.P., Della Pietra, A., 3rd, Diaz, E. et al. (2012) EZH2 inhibition as a therapeutic strategy for lymphoma with EZH2-activating mutations. Nature, 492, 108-112.

31. Hahn, M.A., Hahn, T., Lee, D.H., Esworthy, R.S., Kim, B.W., Riggs, A.D., Chu, F.F. and Pfeifer, G.P. (2008) Methylation of polycomb target genes in intestinal cancer is mediated by inflammation. Cancer Res, 68, 10280-10289.

32. De Santa, F., Totaro, M.G., Prosperini, E., Notarbartolo, S., Testa, G. and Natoli, G. (2007) The histone H3 lysine-27 demethylase Jmjd3 links inflammation to inhibition of polycomb-mediated gene silencing. Cell, 130, 1083-1094.

33. Wang, A., Pan, D., Lee, Y.H., Martinez, G.J., Feng, X.H. and Dong, C. (2013) Cutting edge: Smad2 and Smad4 regulate TGF-beta-mediated Il9 gene expression via EZH2 displacement. J Immunol, 191, 4908-4912.

34. Vella, S., Gnani, D., Crudele, A., Ceccarelli, S., De Stefanis, C., Gaspari, S., Nobili, V., Locatelli, F., Marquez, V.E., Rota, R. et al. (2013) EZH2 down-regulation exacerbates lipid accumulation and inflammation in in vitro and in vivo NAFLD. Int J Mol Sci, 14, 24154-24168.

35. Ezhkova, E., Pasolli, H.A., Parker, J.S., Stokes, N., Su, I.H., Hannon, G., Tarakhovsky, A. and Fuchs, E. (2009) Ezh2 orchestrates gene expression for the stepwise differentiation of tissue-specific stem cells. Cell, 136, 1122-1135.

36. Juan, A.H., Kumar, R.M., Marx, J.G., Young, R.A. and Sartorelli, V. (2009) Mir-214-dependent regulation of the polycomb protein Ezh2 in skeletal muscle and embryonic stem cells. Mol Cell, 36, 61-74.

37. Aljubran, S.A., Cox, R., Jr., Tamarapu Parthasarathy, P., Kollongod Ramanathan, G., Rajanbabu, V., Bao, H., Mohapatra, S.S., Lockey, R. and Kolliputi, N. (2012) Enhancer of zeste homolog 2 induces pulmonary artery smooth muscle cell proliferation. PLoS One, 7, e37712.

38. Hemming, S., Cakouros, D., Isenmann, S., Cooper, L., Menicanin, D., Zannettino, A. and Gronthos, S. (2014) EZH2 and KDM6A act as an epigenetic switch to regulate mesenchymal stem cell lineage specification. Stem cells, 32, 802-815.

39. Pasini, D., Cloos, P.A., Walfridsson, J., Olsson, L., Bukowski, J.P., Johansen, J.V., Bak, M., Tommerup, N., Rappsilber, J. and Helin, K. (2010) JARID2 regulates binding of the Polycomb repressive complex 2 to target genes in ES cells. Nature, 464, 306-310.

SUPPLEMENTAL INFORMATION

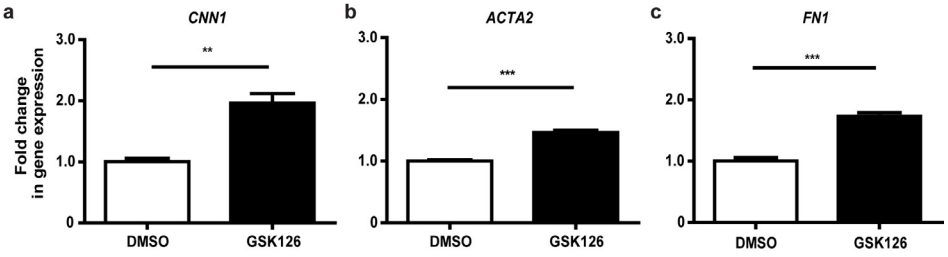

Supplementary Figure 1. Expression of mesenchymal genes upon inhibition of EZH2.
HUVEC were treated with 1μM EZH2 inhibitor GSK126 daily for 4 days. a through c: Fold change in gene expression of *CNN1*, *ACTA2* and *FN1*. **p<0.01, ***p<0.001

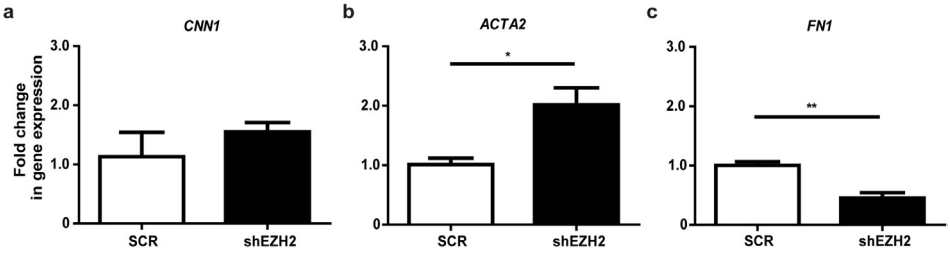

Supplementary Figure 2. Expression of mesenchymal genes upon knock-down of *EZH2*.
HUVEC were depleted of EZH2 by lentiviral overexpression of anti-*EZH2* shRNA. a through c: Fold change in gene expression of *CNN1*, *ACTA2* and *FN1*. **p<0.01, ***p<0.001

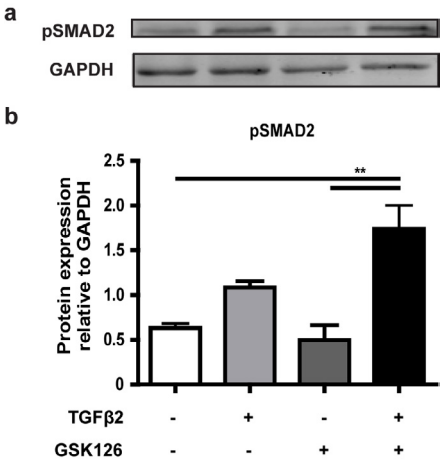

Supplementary Figure 3. Phospho-SMAD2 levels.
HUVEC were treated with the EZH2 inhibitor GSK126 (1μM), or 10ng/ml TGFβ2, or combination of both, daily for 4 days. a: Representative Western blotting results of phosphor-SMAD2 (pSMAD2) expression; GAPDH served as loading control. b: Expression of pSMAD2 derived through densitometry of Western blotting data, normalized to the GAPDH loading control. **p<0.01.